

Waste green sands as reactive media for groundwater contaminated with trichloroethylene (TCE)

Taeyoon Lee^a, Craig H. Benson^{b,*}, Gerald R. Eykholt^c

^a Construction Environment Research Department, Korea Institute of Construction Technology, 2311, Daehwa-Dong, Ilsan-Gu, Goyang-Si, Gyeonggi-Do, 411-712, Republic of Korea

^b Department of Civil and Environmental Engineering, University of Wisconsin-Madison, 2214 Engineering Hall, 1415 Engineering Drive, Madison, WI 53706-1691, USA

^c Eykholt Consulting, 477 Woodside Terrace, Madison, WI 53711-1426, USA

Received 20 August 2003; accepted 6 October 2003

Available online 5 May 2004

Abstract

Waste green sands are byproducts of the gray iron foundry industry that consist of sand, binding agents, organic carbon, and residual iron particles. Because of their potential sorptive and reactive properties, tests were conducted to determine the feasibility of using waste green sands as a low cost reactive medium for groundwater treatment. Batch and column tests were conducted to determine the reactivity, sorptive characteristics, and transport parameters for trichloroethylene (TCE) solutions in contact with green sands. Normalized rate constants for TCE degradation in the presence of iron particles extracted from green sands were found to be comparable to those for Peerless iron, a common medium used to treat groundwater. Rate constants and partition coefficients obtained from the batch tests were found to be comparable to those from the column tests. Analytical modeling shows that reactive barriers containing green sand potentially can be used to treat contaminated groundwater containing TCE at typical concentrations observed in the field.

© 2004 Elsevier B.V. All rights reserved.

Keywords: Foundry byproducts; Beneficial reuse; Sustainability; Reactive barrier; Green sand; Trichloroethylene; Groundwater; Remediation

1. Introduction

Passive in situ treatment of groundwater where contaminants are removed or converted into less toxic or innocuous by-products by interaction with a reactive medium is now an accepted remediation technology. The type of reactive medium that is used depends on the type of contaminants to be treated and the hydrogeological setting. The most common medium is granular zero-valent iron (Fe^0), which has been used to treat chlorinated ethene compounds [1–3], toxic heavy metals [4–7], and chlorinated herbicides [8,9]. Adsorptive media are also used, such as zeolites, straw, wood chips, peat, coal, and tire chips [10–12], as are mix-

tures of granular iron and organic carbon bearing materials [1,13,7,4].

The high capital cost of some in situ treatment technologies can preclude their use at small-contaminated sites. One approach to reduce costs is to use low-cost reactive media such as industrial byproducts that can be obtained for little or no cost [14–16]. The objective of this study was to assess the feasibility of using waste green sands, a byproduct of the gray iron foundry industry, as a low-cost reactive medium for treating groundwater contaminated with TCE. The intent was to use green sands in reactive barriers (RBs), but the material may be applicable to other in situ treatment approaches as well.

Green sands are mixtures of sand, clay binder, and an organic carbon source (typically coal dust) that are used to make molds for iron casting [17]. Most green sands also contain fine iron particles that accumulate during foundry operations. As a reactive medium, the coal dust provides organic carbon for sorption, and the iron particles act as a re-

* Corresponding author. Tel.: +1-608-262-7242; fax: +1-608-263-2453.

E-mail addresses: badger74w@kict.re.kr (T. Lee), benson@engr.wisc.edu (C.H. Benson), geykholt@charter.net (G.R. Eykholt).

ducing agent. Waste green sands generated at foundries are normally disposed in solid waste landfills. Thus, re-using foundry sands as a reactive medium is attractive in terms of sustainable development, and also allows the foundry industry to accrue savings through reduced disposal costs.

Because waste green sands generally are treated as a solid waste, regulations often require that the environmental risks associated with their reuse be considered. In Wisconsin, USA, administrative rules (Section NR 538 of the Wisconsin Administrative Code) provide a framework for evaluating these risks. These rules provide specific criteria regarding leaching of metals and PAHs from green sands in reuse applications. This issue is not addressed in this paper, but is addressed in a leaching study conducted by Lee and Benson [18]. They conducted batch and column leaching tests on a variety of green sands, natural soils, and a commercially available granular iron. Leaching tests on the green sands showed that US groundwater quality standards water were only exceeded for Fe, Cr, and Pb, and that these exceedances were modest (<10%). Moreover, they found that Fe, Cr, and Pb leached at lower concentrations from green sand than from the natural soils and the granular iron that were tested.

2. Materials

2.1. Green sands

Twelve green sands were used in this study. The green sands were obtained from foundries in Wisconsin, Illinois, and Ohio, USA. Index properties of the green sands are summarized in Table 1. Each green sand consists primarily of uniformly graded fine sand. The percent fines (fraction passing the US No. 200 sieve, or 75 μm) ranges from 4.3 to 16.0%, the clay fraction (finer than 2 μm) ranges from 2.9 to 13.2%, and the specific gravity of solids ranges from 2.51 to 2.73. The total organic carbon (TOC) ranges from 0.5

to 4.0%, and the specific surface area of the iron particles extracted from the green sand (measured using the BET method) is 2.45 m^2/g , on average [18].

The saturated hydraulic conductivity of each green sand was measured in a rigid-wall permeameter following the methods described in ASTM D 5886. The constant head method was used and tap water was the permeant liquid. The green sands were tamped into the permeameter with a rod in three layers of equal thickness using 15 tamps per layer. The intent was to create a moderately compacted material that would simulate in situ placement of the sand by loose dumping followed by modest densification. The hydraulic conductivities are summarized in Table 1. They range from 0.00079 m/day to 23.3 m/day, but most are between 0.24 m/day and 1.99 m/day. The broad range in hydraulic conductivity is due to the differences in bentonite content between the sands [18].

Green sands have lower hydraulic conductivity than more common reactive media, such as granular iron, which typically has a hydraulic conductivity on the order of 10 m/day. Thus, green sands might be used in permeable reactive barriers (PRBs) placed in less permeable aquifer materials (fine sands, silty sands), in low-permeability reactive barriers (LPRBs) used in conjunction with groundwater cutoff systems, or other containment scenarios where high flow rates are not anticipated. The hydraulic conductivity of green sands can also be increased to more conventional levels by mixing with coarse materials such as gravel, coarse sand, crushed glass, or tire chips [18]. However, when mixtures are prepared, issues such as faster passivation, alteration of leaching characteristics, segregation, and the additional costs associated with mixing may become important.

2.2. Zero-valent iron

Commercially available zero-valent iron particles were used for comparative tests. The iron particles were obtained

Table 1
Geotechnical properties of the foundry sands

Green sand	Particle size characteristics			USCS classification	Specific gravity of solids	Total organic carbon (%)	Saturated hydraulic conductivity (m/day)
	d_{50} (mm)	Percent fines	2 μm clay content				
1	0.19	10.7	6.7	SP-SM	2.62	1.5	1.35
2	0.19	14.3	9.2	SM	2.53	2.6	1.99
3	0.20	11.3	7.7	SW-SM	2.52	2.5	0.52
4	0.19	13.2	9.3	SC-SM	2.63	0.5	0.00081
5	0.19	12.4	8.0	SC-SM	2.54	1.8	0.24
6	0.28	10.2	5.2	SP-SM	2.61	1.1	0.35
7	0.19	10.9	4.5	SC-SM	2.72	2.2	0.34
8	0.19	11.1	6.2	SP	2.68	2.5	0.0033
9	0.21	4.3	2.9	SP	2.64	0.8	23.3
10	0.19	10.0	3.5	SP-SM	2.73	2.5	0.47
11	0.20	16.0	13.2	SM-SC	2.51	4.0	0.00079
12	0.20	10.0	3.5	SP	2.73	2.4	1.64

Notes: d_{50} , median particle size; percent fines, percent finer than 75 μm ; USCS, unified soil classification system; SP, poorly graded sand; SM, silty sand; SW, well graded sand; and SC, clayey sand.

from Peerless Metal Powders and Abrasives Co. of Detroit, MI, USA. The mean particle size was 0.7 mm and the specific surface area of the iron particles was $0.87 \text{ m}^2/\text{g}$ [19]. The purity of the iron ranged from 92 to 95% by weight. The total carbon content in the iron was 3.5% by weight.

2.3. Chemicals

All chemicals were obtained from Aldrich Chemical Co., Milwaukee, WI, USA. The chemicals included lithium bromide (99% purity), trichloroethylene (TCE) (99.5% purity), and the TCE by-products vinyl chloride (99% purity), 1,1-dichloroethylene (99% purity), *trans*-1,2-dichloroethylene (99% purity), and *cis*-1,2-dichloroethylene (99% purity).

3. Analytical methods

3.1. Total iron content

An acid digestion was conducted on each green sand following USEPA Method 3051 to measure the total iron content. A 0.5-g sample of green sand was digested in 10 ml of concentrated nitric acid for 10 min using a microwave oven. Fluorocarbon digestion vessels were used. Groups of six vessels were evenly located on the turntable in the microwave oven. When less than six vessels were used for digestion, the remaining vessels were filled with nitric acid to ensure that the energy delivered was similar to that applied when six specimens were digested. The vessels were irradiated at 574 W for 10 min. The digestions were diluted to 1 L using Type I DI water, and solids and suspended materials were removed using a $0.45\text{-}\mu\text{m}$ glass fiber filter.

Iron concentrations in the digestions were measured by atomic adsorption using a Varian® SpectrAA 800 following USEPA Method 7000A. Calibration standards were prepared by diluting stock standard solutions purchased from Fisher Scientific, Inc. The calibration standards were acidified using nitric acid to simulate the condition of the digestion solution. Interference effects were compensated by using standard additions as described in Lee and Benson [18]. Total iron contents of the sands typically ranged between 1 and 11%, although two of the sands (9 and 11) had little (<0.2%) iron.

3.2. Total organic carbon

Total organic carbon (TOC) content of each green sand was measured using a Lab 2100 TOC analyzer (Zellweger Analytix). Inorganic carbon existing in the form of calcite or dolomite was removed beforehand by adding 4 M HCl as described in *Methods of Soil Analysis* [21].

3.3. TCE and TCE byproducts

Concentrations of TCE and the TCE byproducts were measured using a Varian 3600 gas chromatograph (GC)

equipped with an OI analytical discrete purging multisampler (DPM-16), an OI analytical multiple heater controller (MHC-16), and a Model 4560 purge-and-trap sample concentrator. A Supelcowax-10 megabore column ($60 \text{ m} \times 0.25 \text{ mm}$ inside diameter) and flame-ionization detector (FID) were installed on the GC. Standards for calibration were prepared gravimetrically from stock solutions. All calibration curves were based on four standards prepared over the range of expected concentrations. The detection limit (DL) was $15 \mu\text{g/L}$ for TCE, $10 \mu\text{g/L}$ for 1,1-dichloroethylene (1,1-DCE), $12 \mu\text{g/L}$ for *trans*-1,2-dichloroethylene (*trans*-DCE), and $9 \mu\text{g/L}$ for *cis*-1,2-dichloroethylene (*cis*-DCE). Reliable detection of vinyl chloride was not possible with the purge-and-trap method that was used.

Liquid from the batch and column tests was sampled using a $100\text{-}\mu\text{L}$ gas-tight syringe and then directly injected into multisampler tubes. To ensure complete purging, the multisampler tubes were heated to 75°C for 2 min before purging and for 11 min during purging. The column temperature was held at 40°C for 2 min and then raised to 50°C at a gradient of $1.0^\circ\text{C}/\text{min}$. The temperature was then increased to 225°C at a gradient of $40.0^\circ\text{C}/\text{min}$ and then held for 2.5 min to remove any residuals in the column.

3.4. Bromide tracer analysis

Tracer tests were conducted using a bromide solution to determine the effective porosity. The bromide solution was used as influent after the TCE breakthrough curves were complete. Concentrations of bromide were measured using a Beckman System Gold High Performance Liquid Chromatograph (HPLC) with a conductivity detector. The HPLC column was 150 mm in length and 4.6 mm in diameter, and contained Universal Anion 10 u. The column temperature was maintained at 45°C during the analysis. Calibration was performed using 1, 3, 5, 10, and 20 mg/L bromide solutions prepared with Type I DI water. The standard solution was delivered at a flow rate of 1 mL/min. The DL for bromide was determined to be 0.5 mg/L.

4. Batch and column test methods

4.1. TCE solution preparation

A designated amount of TCE liquid was extracted using a gas-tight syringe and injected into a 2-L volumetric flask filled with Type I DI water. The Type I DI water was sparged beforehand with nitrogen gas for 1 h to remove dissolved oxygen, and mixed with sodium azide (0.1% by weight) to prevent biological activity. The solution was mixed with a magnetic stirring bar for 10 h. Aliquots of TCE ($100 \mu\text{L}$) were analyzed to evaluate losses during preparation. The variation was $\pm 4\%$ of the expected value for TCE, which suggests that losses during preparation were minimal.

4.2. Batch sorption tests

Batch sorption tests were conducted to evaluate sorption of TCE onto the green sands. A constant dry mass of green sand (5 g) was used with initial TCE concentrations ranging between 1 and 40 mg/L. Iron in the sand was removed with a magnet before testing. Partition coefficients were obtained by fitting the sorption data with linear and Freundlich isotherm models using a least-squares algorithm.

The TCE solutions were placed with green sand into 40 ml Teflon® bottles sealed with Teflon® caps. The bottles were tumbled at 30 rpm. Solutions with no green sand were used as controls to estimate losses. Final concentrations of the controls were assumed to be the initial concentration of the mixtures to account for losses during the test, as suggested by Zytner [22]. After tumbling, the liquid and solid phases were separated by centrifugation at 8000 rpm and 4 °C.

A series of batch tests was initially conducted to evaluate the required tumbling time and sorption kinetic behavior of TCE (35 mg/L) with green sands. Green sands without iron were used that had TOCs between 0.8 and 4.0% and clay contents between 2.9 and 13.2%. Vials with identical contents were used, and TCE concentrations were measured at various tumbling times. For all tests, the TCE concentration stabilized by 20 h [18]. Thus, a tumbling time of 24 h was used for all subsequent tests to ensure equilibrium was attained.

4.3. Batch degradation tests

Batch tests were conducted with green sand iron or Peerless iron to evaluate reactivity of the iron. Iron particles were extracted from the green sands using a magnet, washed with methanol, and then dried for 5 min with a heater set at 40 °C. No brown oxides (e.g. iron oxyhydroxides) were visible on the washed particles. The Peerless iron particles were washed using the same procedure. After drying, the iron particles (1, 2, 4, or 8 g) were placed in 50 ml screw-capped glass VOC vials each equipped with a Teflon®-coated septum. The vials were filled with TCE solution to the top to eliminate headspace. Vials without iron particles were used as controls. All vials were tumbled at 30 rpm. At the designated sampling time, a sacrificial vial was removed from the tumbler, allowed to sit for 5 min to settle the iron particles, and then a sample was collected using a 100- μ L gas-tight syringe by piercing the Teflon®-coated septum.

A first-order decay model with instantaneous sorption from Koppensteiner [9] was used to determine the bulk reaction rate constant (K_{obs}) and the iron-phase partition coefficient for TCE (K_{pi}). The model is:

$$C_{aq}(t) = \frac{C_0}{K_{pi}S_r + 1} \exp\left(-\frac{K_{obs}t}{K_{pi}S_r + 1}\right) \quad (1)$$

where C_{aq} is the concentration of TCE in the batch reactor at time t (mg/L), C_0 is initial TCE concentration (mg/L), and S_r is solid-solution ratio (kg/L). Eq. (1) was fit to the data using

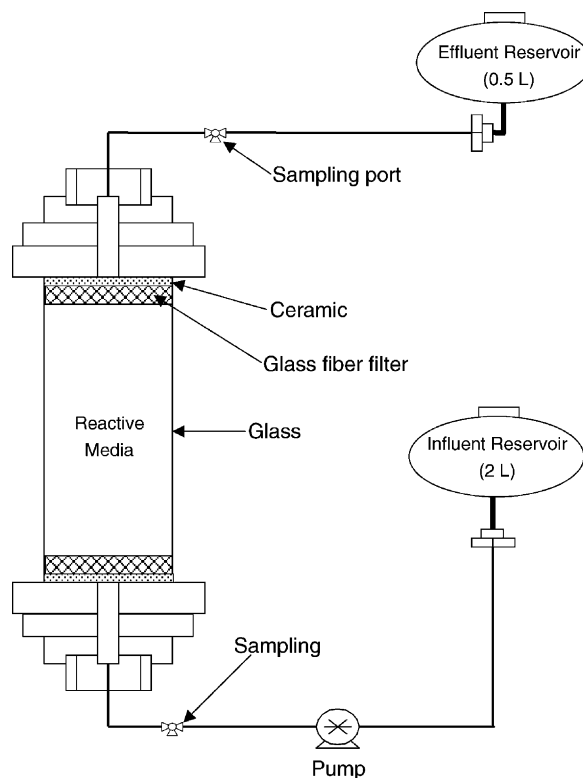


Fig. 1. Schematic of column test apparatus.

a non-linear least-squares algorithm to obtain K_{obs} (h^{-1}) and K_{pi} (L/kg).

4.4. Column tests

Column tests were conducted to determine partition coefficients and rate constants under conditions simulating flow through a porous medium. A schematic of the column test set-up is shown in Fig. 1. The reactive material was contained in a glass cylinder with a porous ceramic disk at each end. A glass fiber filter was placed between the porous disk and the test medium.

Green sand was tamped into the glass column with a rod in three layers of equal thickness using 15 tamps per layer. The specimens were then permeated with Madison tap water for at least two pore volumes of flow. Afterwards, the influent solution was switched to TCE solution for the column test. After finishing the column tests with TCE, a lithium bromide solution (20 mg/L) was introduced into the column as a tracer to determine the effective porosity and the dispersivity.

The TCE solution used as influent was contained in a 2-L Teflon® bag submerged in water to minimize losses from diffusion. The TCE concentration in the bag was periodically measured and the variation in concentration was found to be $\pm 5\%$ of the expected TCE concentration. The solution was delivered into the bottom of the column (i.e., upward flow) using a peristaltic pump at flow rates varying between

20 and 60 mL/h. The bromide solution was delivered in the same manner.

An analytical solution of the advection-dispersion-reaction equation (ADRE) provided by van Genuchten [23] was fitted to the column test data:

$$\frac{C_e}{C_0} = \frac{1}{2} \left[\exp\left(\frac{(v-u)L}{2D}\right) \operatorname{erfc}\left(\frac{RL-ut}{2(DRt)^{1/2}}\right) \right] + \frac{1}{2} \left[\exp\left(\frac{(v+u)L}{2D}\right) \operatorname{erfc}\left(\frac{RL+ut}{2(DRt)^{1/2}}\right) \right] \quad (2)$$

where C_e is the time-varying concentration at the effluent end of the column, C_0 is the constant influent concentration, L is the column length, v is the seepage velocity, D is the dispersion coefficient, and R is the retardation factor. The concentrations C_0 and C_e were measured at the sampling ports shown in Fig. 1. Eq. (2) is for the first-type initial and boundary conditions (i.e., the background concentration is zero, the influent concentration is constant, and the concentration gradient is zero at great distance from the influent boundary). The variable u in Eq. (2) is defined as:

$$u = v \left(1 + \frac{4K_{\text{obs}}D}{v^2} \right)^{1/2} \quad (3)$$

Use of Eq. (3) implicitly assumes that degradation of adsorbed TCE is negligible. The retardation factor is related to the bulk partition coefficient (K_p) for the linear isotherm via:

$$R = 1 + \frac{\rho_d}{n} K_p \quad (4)$$

where ρ_d is the dry density and n is the porosity. For the steady-state condition, the effluent concentration (C_{SS}) is:

$$C_{SS} = C(L, \infty) = C_0 \exp\left[\frac{(v-u)L}{2D}\right] \quad (5)$$

The dispersion coefficient (D) obtained by fitting Eq. (2) to the column test data is the sum of the mechanical dispersion coefficient (D_m) and the molecular diffusion coefficient (D^*):

$$D = D_m + D^* \quad (6)$$

The mechanical dispersion coefficient D_m can be related to the seepage velocity via:

$$D_m = \alpha_L v^m \quad (7)$$

where α_L is the longitudinal dispersivity and m is an empirical constant that typically is assumed to be unity for granular media [24]. When analyzing the column data, m was assumed to be unity and D^* was assumed to be negligible because transport in the columns was dominated by advection.

5. Results of batch tests

5.1. Batch sorption tests

Isotherms from the batch sorption tests are shown in Fig. 2. All tests had approximately linear isotherms in the range of the equilibrium concentrations that were considered. However, significant non-linearity may occur at lower concentrations (<1 mg/L) since many of the linear isotherms appear to have a y-intercept greater than zero.

Parameters obtained by fitting the linear and Freundlich models to the data are summarized in Table 2. Fits of the linear isotherm were made with a non-zero intercept and the intercept forced to zero. Slightly better fits were obtained with the Freundlich isotherm ($R^2 = 0.73$ – 0.98) than with the linear isotherm with no intercept constraint ($R^2 = 0.76$ – 0.98), but both models provide a good description of the data in the range of concentrations that were used. Poorer fits were obtained with the linear model forced through the origin ($R^2 = 0.70$ – 0.94), which reflects the non-linearity expected at low concentrations. Most sands exhibit slight convex non-linearity (i.e., $n > 1$) with the Freundlich model,

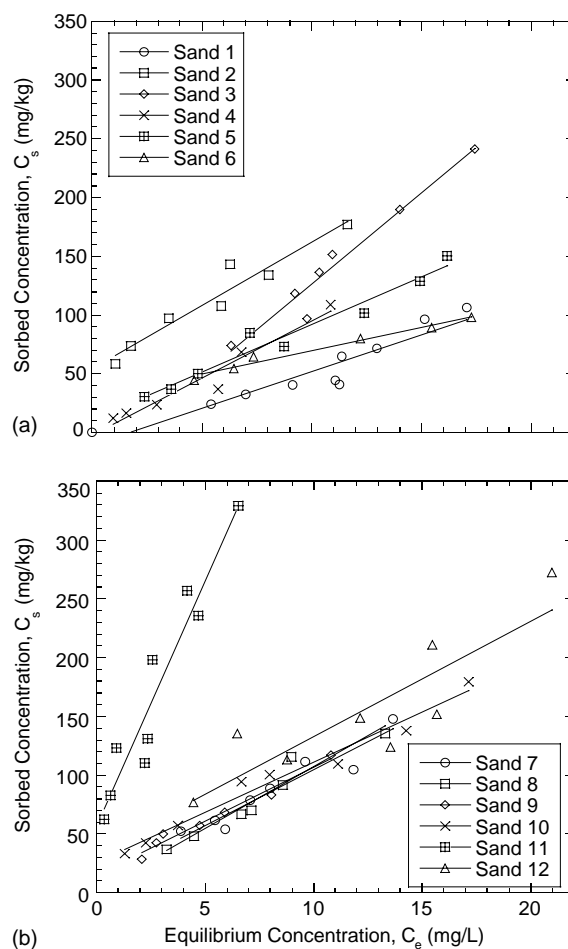


Fig. 2. TCE sorption isotherms from batch tests conducted with green sands: (a) Sands 1–6 and (b) Sands 7–12.

Table 2
Partition coefficients from batch sorption tests

Green sand	Linear isotherm				Freundlich isotherm		
	No Intercept Constraint		Intercept forced to zero		K_f (L/kg)	n	R^2
	K_p (L/kg)	R^2	K_p (L/kg)	R^2			
1	5.4	0.82	5.4	0.82	3.64	0.92	0.93
2	10.8	0.94	17.9	0.36	56.4	2.27	0.96
3	15.6	0.96	13.1	0.93	9.1	0.88	0.92
4	9.7	0.95	9.4	0.94	10.9	1.14	0.94
5	8.1	0.96	9.1	0.94	13.9	1.20	0.97
6	4.0	0.98	6.3	0.57	18.9	1.72	0.98
7	9.5	0.91	10.5	0.90	14.8	1.18	0.90
8	10.5	0.94	10.7	0.94	11.4	1.03	0.96
9	9.2	0.98	11.3	0.90	18.6	1.33	0.96
10	8.5	0.97	10.7	0.88	23.9	1.49	0.99
11	41.6	0.92	55.5	0.77	106.5	1.92	0.88
12	9.8	0.76	12.2	0.70	31.3	1.56	0.73

Note: R^2 , coefficient of determination from regression analysis.

which also suggests greater affinity for TCE at low concentrations than at higher concentrations. This behavior is characteristic of carbonaceous materials with high surface area such as the powdered “sea coal” additive in green sands [26].

Partition coefficients obtained from the batch sorption tests are shown as a function of TOC in Fig. 3. For intermediate TOC (1–3.5%), which are characteristic of most foundry sands (Table 1), K_p and TOC are approximately linearly related. This relationship can be described by:

$$K_p = 4.76 \text{ TOC} \quad (8)$$

where K_p is in L/kg and TOC is in percent. For both the low and high TOC ranges, the K_p are higher than those predicted by Eq. (8). These higher K_p are believed to be due to the high clay content and presence of organic binder in some of the sands. Sand 4 (TOC = 0.5% and K_p = 9.7 L/kg) and Sand 11 (TOC = 4.0% and K_p = 41.6 L/kg) both have a clay content in excess of 10%, which may provide additional sorption sites for TCE. Sand 9 (TOC = 0.8%, clay content = 2.9%, and K_p = 9.2 L/kg) includes an organic additive for binding the sand particles that is not present in the other sands, which also may be responsible for the additional sorptive capacity.

The linear relationship between K_p and TOC for intermediate TOCs suggests that empirical methods used to estimate K_p for organic chemicals and organic-carbon bearing soils (e.g., [27–29]) might be useful for estimating K_p for green sands. These methods assume that K_p equals the product of the organic carbon fraction ($f_{OC} = \text{TOC}/100$) and the organic carbon partition coefficient (K_{OC}), the latter typically being estimated using an empirical expression based on the octanol-water partition coefficient (K_{OW}) or solubility (S). The K_{OC} for green sands with intermediate TOC is 476 L/kg, whereas estimates of K_{OC} based on K_{OW} and S for TCE yield K_{OC} ranging between 157 and 209 L/kg [27–29]. That is, the K_{OC} computed from the batch test data are more than a factor of two higher than the range of K_{OC} estimates.

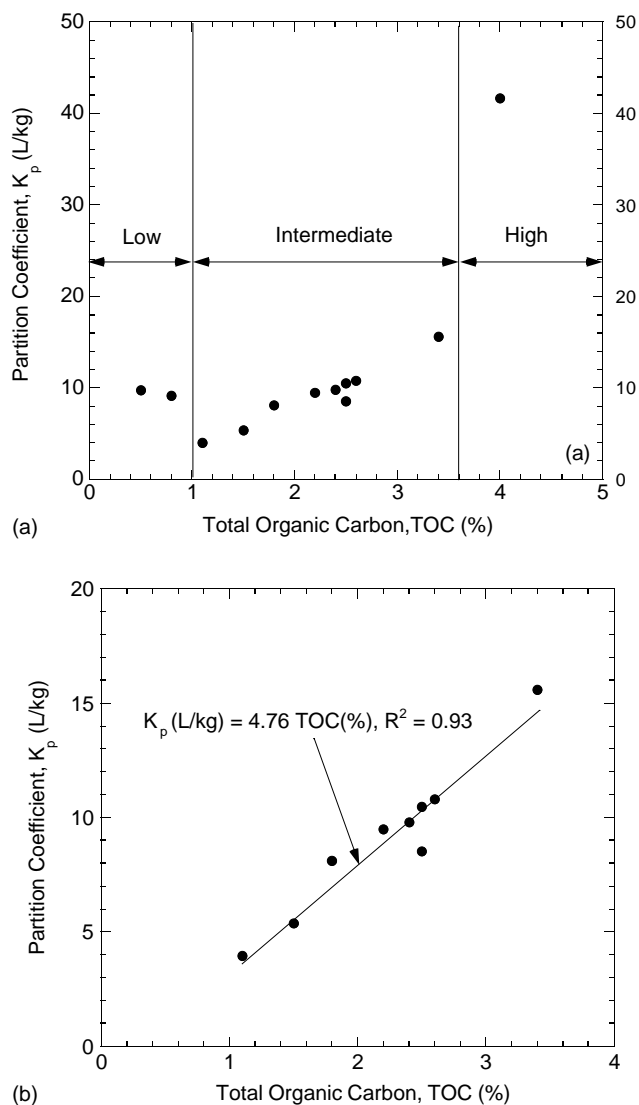


Fig. 3. Relationship between K_p and TOC: (a) full range of TOC and (b) intermediate range of TOC.

Table 3
Experimental conditions, rate constants, and partition coefficients for batch degradation tests

Test	Iron source	Initial conc. (mg/L)	Iron surface area/volume (m^2/L)	Dissolved oxygen (mg/L)	NaCl (M)	Rate constant ($\text{L}/\text{m}^2 \text{ h}$)	Partition coefficient (L/kg)
A	Green Sand	5.2	54	5.4	0.00	2.37×10^{-4}	2.13
B	Green Sand	31.9	57	<0.6	0	1.02×10^{-4}	1.22
C	Green Sand	31.9	58	5.4	0.02	1.03×10^{-4}	0.77
D	Green Sand	8.8	58	<0.6	0	1.14×10^{-4}	1.76
E	Green Sand	15.2	86	6.0	0	2.06×10^{-4}	1.72
F	Green Sand	40.3	125	5.8	0	1.17×10^{-4}	2.41
G	Peerless Iron	40.3	22	5.6	0	1.76×10^{-4}	2.12
H	Peerless Iron	40.3	44	5.6	0	1.65×10^{-4}	1.79
I	Peerless Iron	40.3	89	5.6	0	1.71×10^{-4}	1.52
J	Peerless Iron	40.4	180	5.6	0	1.72×10^{-4}	1.61

The reason for the higher K_{OC} is not apparent. The organic carbon in green sands may differ from that normally found in soils, or additional mechanisms may be contributing to TCE adsorption in green sands (e.g., sorption on the mineral solids). Nevertheless, comparison of the measured and estimated K_{OC} suggests that the common empirical methods to estimate K_p for organic chemicals and soil can be used conservatively for green sands.

5.2. Batch degradation tests

Six sets of batch tests (Tests A–F) were conducted to evaluate degradation rates for TCE in the presence of iron particles from the green sands. Four other tests (Test G–J) were conducted using Peerless iron particles for comparison. All tests were performed at room temperature ($23 \pm 2^\circ\text{C}$), under a variety of conditions (Table 3). The range of initial TCE concentrations was 5.2–40.4 mg/L, which was selected to represent typical TCE concentrations in groundwater at contaminated sites [30–34]. Two levels of dissolved oxygen concentration (DO) were used to simulate typical groundwater conditions. In many cases where VOCs contaminate groundwater, the dissolved oxygen (DO) concentration in groundwater is very low. However, modest DO concentrations have been reported for contaminated groundwater near the ground surface [31]. Tests with high DO were conducted using unprocessed DI water, which had DO of 5.4 and 6.0 mg/L. Tests with low DO were conducted using DI water purged with N_2 gas for 20 min, which resulted in DO concentrations less than 0.6 mg/L. One test was spiked with NaCl (0.02 M) to estimate the influence of chloride ion, which accelerates oxidation of iron [35].

Concentrations from the batch degradation tests are shown in Fig. 4 for tests conducted with green sand iron (Fig. 4a) and Peerless iron (Fig. 4b) along with fits of Eq. (1). The rate constants and iron partition coefficients are summarized in Table 3. The rate constants in Table 3 (K_{SA}) are normalized by the ratio of iron surface area to solution volume (SSA); i.e., $K_{SA} = K_{obs}/\text{SSA}$.

The iron surface area to solution volume ratio (SSA) was varied between $54 \text{ m}^2/\text{L}$ and $125 \text{ m}^2/\text{L}$ to determine if the

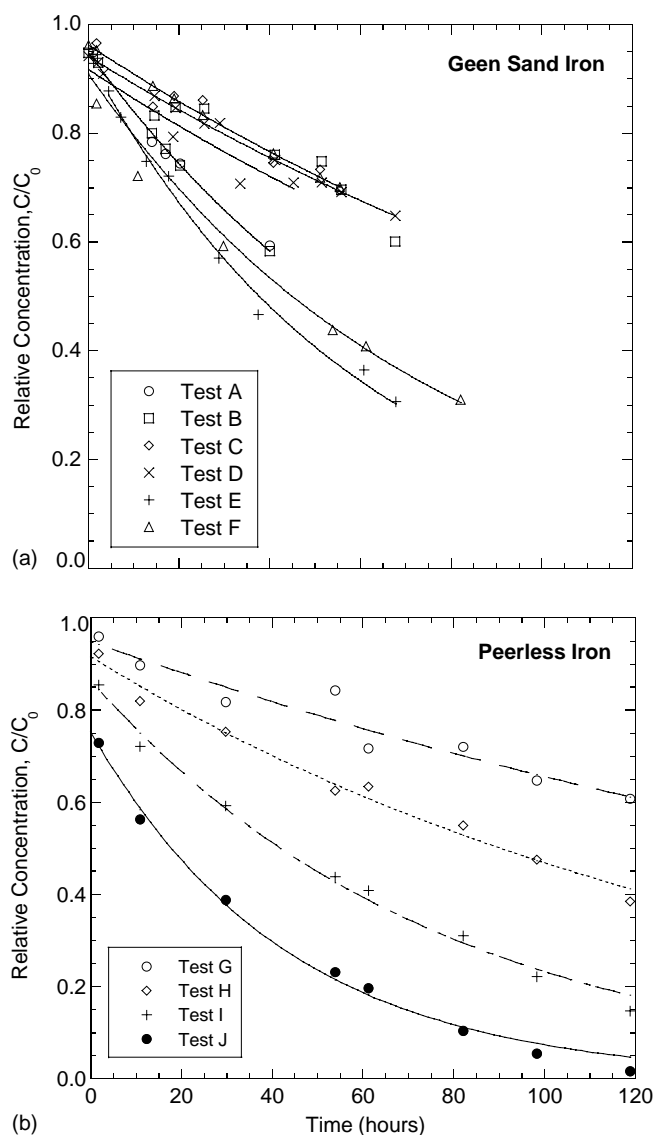


Fig. 4. Relative TCE concentrations as a function of time from batch degradation tests: (a) green sand iron and (b) Peerless iron.

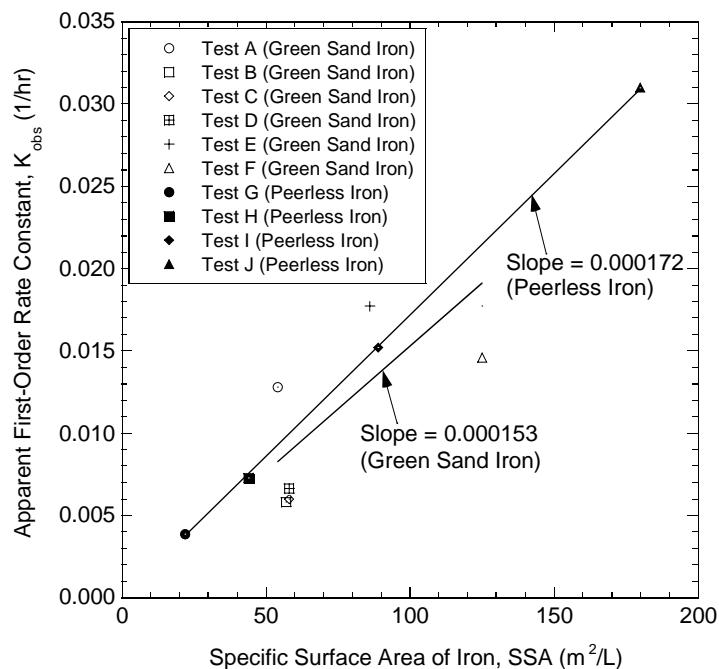


Fig. 5. Apparent first-order rate constant (K_{obs}) as a function of specific surface area (SSA) of green sand iron and Peerless iron.

rate constant for green sand iron could be normalized by SSA as is done for commercially available iron [36]. As shown in Fig. 5, the bulk first-order rate constant, K_{obs} , is approximately linearly proportional to specific surface area (SSA) for the data obtained from Peerless iron. There is more scatter for the green sand iron, but the trend line fit through the green sand data has essentially the same slope as that for Peerless iron. The slope in Fig. 5 is equal to the average normalized rate constant (K_{SA}), which is $1.72 \times 10^{-4} \text{ L/m}^2 \text{ h}$ for Peerless iron and $1.53 \times 10^{-4} \text{ L/m}^2 \text{ h}$ for green sand iron. Therefore, the reactivity of green sand iron appears comparable to that of Peerless iron. Evaluation of the K_{SA} reported in Table 3 also suggests the normalized rate constant and the partition coefficient do not depend significantly on the initial TCE concentration, dissolved oxygen concentration, or the presence of chloride ion.

Analyses were conducted for the TCE by-products (1,1-DCE, *trans*-1,2-DCE, and *cis*-1,2-DCE) to confirm that the dechlorination reaction was occurring. No *trans*-1,2-DCE was detected. Concentrations of 1,1-DCE and *cis*-1,2-DCE from Test F (green sand iron, $\text{SSA} = 125 \text{ m}^2/\text{L}$) and Tests I–J (Peerless iron, $\text{SSA} = 89\text{--}180 \text{ m}^2/\text{L}$) are shown in Fig. 6. The concentrations of 1,1-DCE are lower than 0.06 mg/L for both green sand iron and Peerless iron, except for one data point from Test J (Peerless iron), which was 0.18 mg/L . The concentrations of *cis*-1,2-DCE from the tests with green sand iron and Peerless iron are also comparable, and are appreciably higher than the 1,1-DCE concentrations. Similar concentrations of 1,1-DCE and *cis*-DCE from the tests with green sand iron and Peerless iron suggest that the rate constants for both types of iron for TCE are comparable.

6. Results of column tests

Four green sands were selected for column testing (Sands 1, 9, 11, and 12). The experimental conditions are summarized in Table 4. Sands 1 and 12 were selected to represent green sands bracketing the range of typical iron contents (2.8% for Sand 1 and 11.2% for Sand 12). Sands 9 and 11, which contain little iron ($<0.2\%$), were selected to evaluate partitioning independent of iron-mediated degradation. Sand 11 was mixed in equal proportions with silica sand (50/50 by weight) to increase its hydraulic conductivity. A control test was also conducted.

6.1. Control test

A control column test was conducted with a uniformly graded clean quartz sand to assess sorption on the tubes and glass column. The sand had a median particle size of 0.2 mm , a coefficient of uniformity of 2.6, and a coefficient of curvature of 0.84. The sand was washed with DI water beforehand, and then packed in the glass column using the same procedure used for the reactive materials.

Breakthrough data for TCE from the control test are shown in Fig. 7 along with a fit of Eq. (2) using R and D as the fitting parameters. To avoid problems with non-uniqueness, the effective porosity was fixed at 0.33, which was obtained from a tracer test. The partition coefficient was computed from R using Eq. (4).

The breakthrough curve reached steady state at $C/C_0 = 1$, indicating that no continuous loss was occurring. The partition coefficient for TCE obtained from the control test was 0.79 L/kg . The modest amount of partitioning that occurred

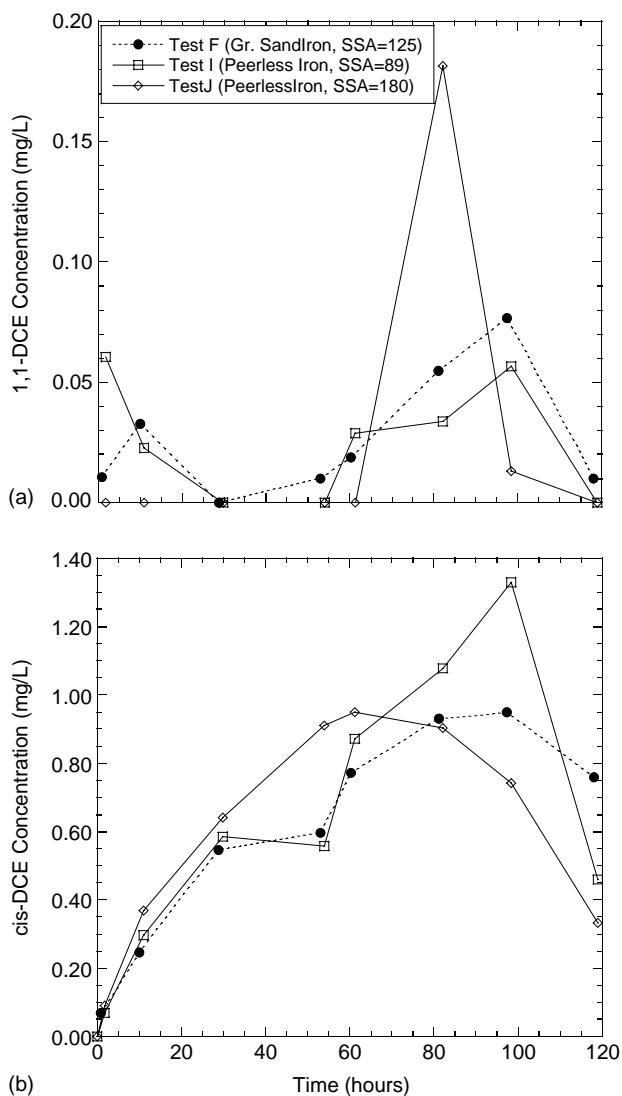


Fig. 6. Concentrations of 1,1-DCE and *cis*-DCE produced from reduction of TCE during batch degradation tests.

is believed to be due to organic carbon in the sand. To assess this hypothesis, K_p was estimated using the organic carbon fraction of the sand ($f_{oc} = 0.0004$) and the empirical equation reported by Shimizu et al. [29]:

$$K_p = f_{oc} 10^{A \log K_{ow} + B} \quad (9)$$

where A and B are empirical constants. The empirical constants A and B were set at 0.98 and -0.26 , as re-

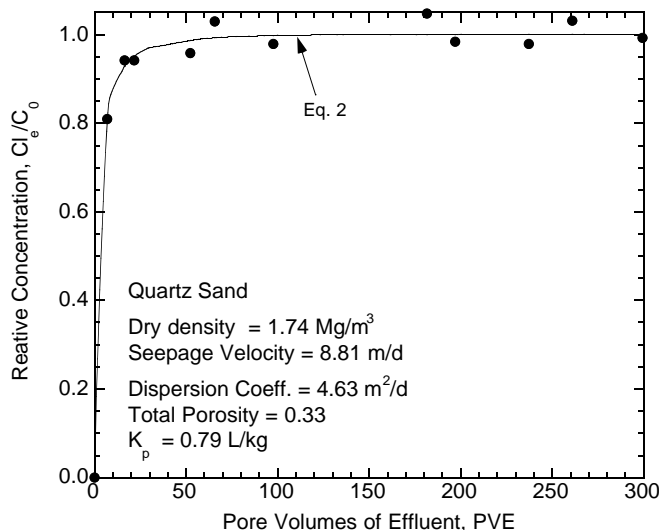


Fig. 7. TCE concentrations and fit of Eq. (3) for a TCE control column test with quartz sand.

ported in Shimizu et al. [29]. The K_p for TCE estimated with Eq. (9) is 0.66 l/kg, which is close to the measured K_p (0.79 L/kg). Therefore, sorption onto the column materials is believed to be minimal, and no correction for losses was made for the column tests with reactive media.

6.2. Effective porosity and dispersion coefficient

Effective porosities and dispersion coefficients were obtained by fitting Eq. (2) to the breakthrough data from the tracer tests assuming $K_{obs} = 0$ and $R = 1$. The effective porosity was calculated by dividing the measured specific discharge by the seepage velocity obtained from the fit. Longitudinal dispersivity was calculated using Eq. (7). The longitudinal dispersivities and effective porosities are summarized in Table 4. The longitudinal dispersivities are close to 0.1 L. The effective porosities (n_e) are comparable to, but tend to be slightly greater than the total porosities (n) determined by weight-volume calculations (the effective porosity ratio, n_e/n , ranges from 0.95 to 1.18). Swelling of the clay fraction in the column may have attributed to the effective porosities being slightly larger than the total porosities. Regardless, the effective porosity ratios fall in the typical range for compacted finer textured soils [37,38].

Table 4
Test conditions and transport parameters for column tests conducted with TCE and LiBr tracer

Green sand	Dry density (mg/m ³)	Seepage velocity (m/day)	Total porosity (n)	Effective porosity (n_e)	n_e/n	Dispersivity (m)		K_p (L/kg)	K_{obs} (1/h)	SSA (m ² /L)	K_{SA} (L/m ² h)
						Measured	0.1L				
1	1.68	1.04	0.36	0.37	1.03	0.040	0.027	9.1	0.063	327	0.000193
9	1.63	2.07	0.39	0.46	1.18	0.014	0.043	7.23	–	0.0	–
11	1.49	4.32	0.43	0.46	1.07	0.100	0.030	41.0	–	0.0	–
12	1.60	0.86	0.39	0.37	0.95	0.052	0.029	10.9	0.126	1034	0.000122

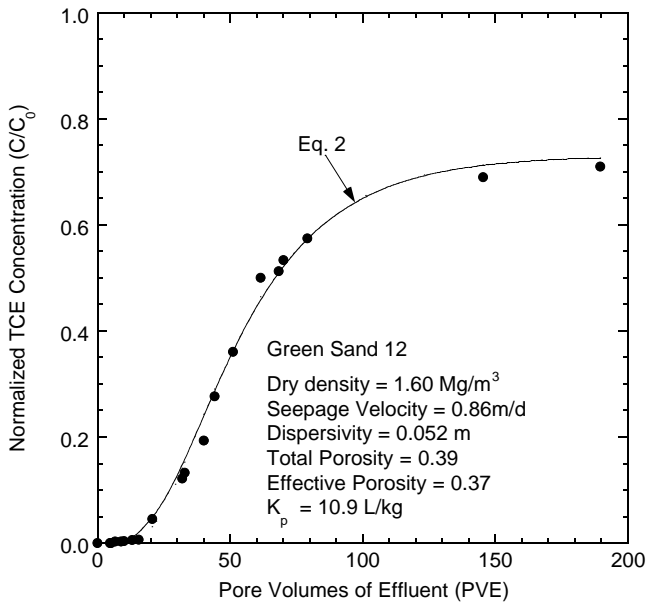


Fig. 8. TCE breakthrough curve and fit of Eq. (3) for green sand 12.

6.3. Partition coefficient and first-order rate constant

To avoid problems with non-uniqueness when analyzing the TCE breakthrough data, the seepage velocity and dispersion coefficient were fixed based on the results of the tracer analysis and the variables u and R in Eq. (2) were used as fitting parameters. A typical fit of Eq. (2) made in this manner is shown in Fig. 8. The normalized rate constant (K_{SA}) was computed as the ratio K_{obs}/SSA and Eq. (4) was used to compute the partition coefficient from R . The partition coefficient for the test using Sand 11 (i.e., the 50–50 mixture of green sand and silica sand) was computed by multiplying the partition coefficient obtained from Eq. (5) by two under the assumption that sorption of TCE on the silica sand is negligible. A summary of the transport parameters is in Table 4.

Partition coefficients from the column tests are graphed against those from the batch sorption tests in Fig. 9. The partition coefficients from both tests are comparable, suggesting that batch tests provide reasonable estimates of the partition coefficient of green sands for flow-through conditions. Similarity of the partition coefficients also suggests that rate-limited sorption was not significant.

The rate constants are tabulated in Table 4. Similar normalized rate constants (K_{SA}) were obtained for Sands 1 and 12, even though they are from different foundries in different states. The average K_{SA} from the green sand column tests is $1.6 \times 10^{-4} \text{ L/m}^2 \text{ h}$, whereas the batch tests yielded $1.5 \times 10^{-4} \text{ L/m}^2 \text{ h}$ for green sand and $1.7 \times 10^{-4} \text{ L/m}^2 \text{ h}$ for Peerless iron (Fig. 5). That is, the K_{SA} obtained from the batch and column tests on green sands are similar, and approximately the same as the K_{SA} for Peerless iron. Thus, batch tests also appear to provide reasonable estimates of the K_{SA} of green sands for flow-through conditions.

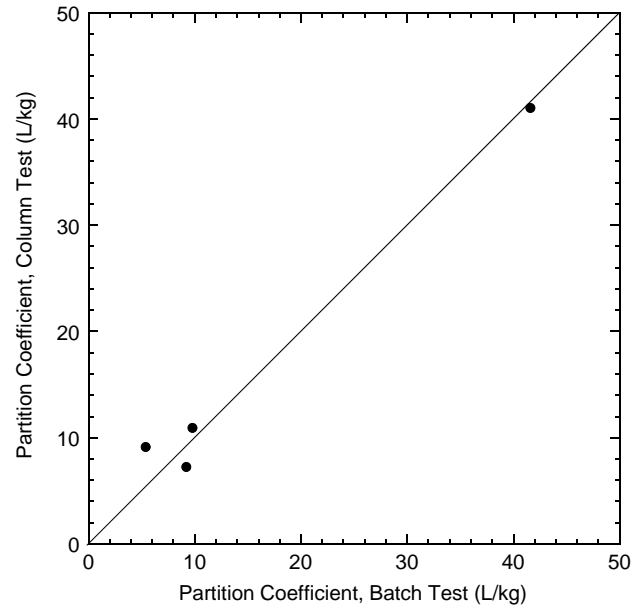


Fig. 9. Partition coefficients obtained from batch sorption and column tests.

The average K_{SA} for the green sand is also comparable to values reported by Johnson et al. [36] and Sivavec et al. [39] for commercially available granular iron. Johnson et al. [36] report K_{SA} of 0.3×10^{-4} to $7.5 \times 10^{-4} \text{ L/m}^2 \text{ h}$ for a variety of granular irons based on data obtained from batch and column tests. Sivavec et al. [39] report K_{SA} between 0.6×10^{-4} and $1.2 \times 10^{-4} \text{ L/m}^2 \text{ h}$ for Peerless iron from column tests.

7. Practical implications for barrier design

7.1. Barrier thickness

Computations were made using Eq. (5) to illustrate typical barrier thicknesses that would be required for RBs constructed with green sands. The dispersion coefficient was computed using Eqs. (6) and (7) using a dispersivity equal to 0.1 times the barrier thickness. The molecular diffusion coefficient for TCE in a porous medium was set at $3.3 \times 10^{-6} \text{ cm}^2/\text{s}$, assuming a tortuosity of 0.40 and an aqueous diffusion coefficient of TCE = $8.6 \times 10^{-6} \text{ cm}^2/\text{s}$ [40]. To bracket common field conditions [4,20,25,30–34,41], the seepage velocity was set at 0.1 m/day and 1 m/day and the influent TCE concentration (C_0) was assumed to be 0.4 or 400 mg/L. For these concentrations, the normalized concentration of TCE (C/C_0) required to meet the maximum contaminant level (MCL) ($C = 0.005 \text{ mg/L}$) is 0.0125 and 0.0000125.

The iron content was varied from 0.1 to 10% to bracket typical iron contents for green sands. Typical values were assumed for dry density (1.5 mg/m^3) and specific gravity of solids (2.62) when calculating the SSA. The bulk first-order

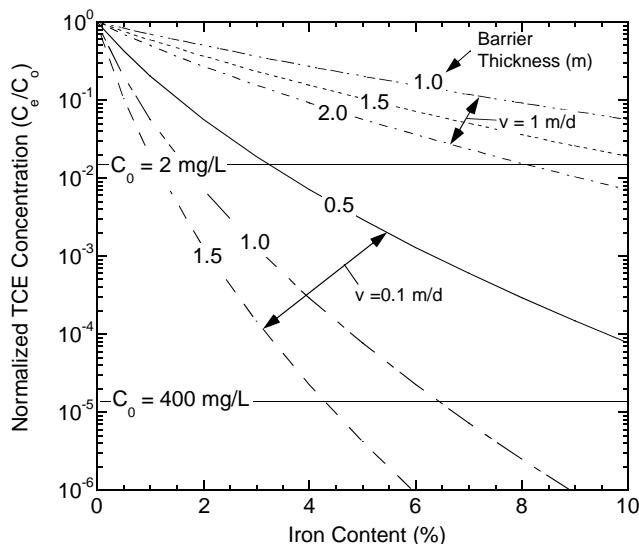


Fig. 10. Normalized TCE concentration in effluent as a function of iron content and barrier thickness for seepage Velocities = 0.1 and 1 m/day.

rate constant was calculated by multiplying the SSA for a given iron content by the average K_{SA} for the green sands ($1.6 \times 10^{-4} \text{ L/m}^2 \text{ h}$) obtained from the column tests.

Normalized TCE concentrations are shown in Fig. 10 for various iron contents and barrier thicknesses. PRBs less than 1 m wide appear practical for lower seepage velocities ($<0.1 \text{ m/day}$) and modest iron contents. At high seepage velocities (1 m/day), achieving the MCL may not be practical unless a thick barrier with high iron content is used and the TCE concentration in the inflowing groundwater is low. Thus, green sands may not be practical at sites where groundwater velocities and TCE concentrations are high. Moreover, the lower hydraulic conductivity of green sands relative to conventional RB media may render green sands more suitable at sites where the seepage velocity is lower.

7.2. Other issues

There are other practical issues that need to be resolved if green sands are used for reactive barriers. For example, little is known about the long-term reactivity of the iron in green sands. Other issues that need to be considered include in situ leaching characteristics, availability and fluctuations in the green sand supply, transportation costs to the project site, variability in the properties of green sands (e.g., due to variations in foundry operations), and degradation of the byproducts of TCE reduction. Some of these issues can be addressed using existing data. For example, long-term tests conducted by Lee and Benson [18] have shown that the rate constant for reduction of the herbicide metolachlor remained within a factor of 1.5 of its initial value after permeation of columns containing green sand or granular iron for 1500 pore volumes of flow. Other issues need to be evaluated by additional study or on a site specific basis. Examples of site-specific issues include the potential for addi-

tional costs incurred by constructing a thicker barrier using green sands (relative to a barrier constructed with granular iron) and regulatory hurdles associated with using an industrial byproduct in an application below the groundwater table.

8. Summary and conclusions

The objective of this study was to evaluate the potential of using waste green sand from gray iron foundries as an inexpensive reactive medium for treating groundwater contaminated with TCE. Batch and column tests were conducted to evaluate the reactivity and sorptive capacity of twelve green sands for TCE.

Results of the tests showed that green sands have a high sorption capacity for TCE, with partition coefficients ranging from 4.0 to 41.6 L/kg. A linear sorption model can be used to describe the sorption isotherms when the TCE concentrations are modest (i.e., 1 to 40 mg/L). When the concentration is lower than 1 mg/L, the partition coefficient is likely to be larger than that indicated by the linear model. Partition coefficients obtained from the column tests were found to be similar to those obtained from batch tests. Therefore, linear isotherms derived from batch tests appear to be reliable for describing partitioning for flow-through conditions.

Normalized degradation rate constants obtained from the batch tests were similar for green sand iron and Peerless iron, which suggests that the iron in green sands has comparable reactivity as commercially available granular iron. The normalized rate constants for green sand iron obtained from the column tests were also similar to those from the batch tests, indicating that the rate constants from batch tests are representative of flow-through conditions.

Calculations showed that the required thickness of a RB constructed with green sand depends on the source TCE concentration and the iron content in the green sand. For source TCE concentrations less than 400 mg/L and seepage velocities less than 0.1 m/day, RBs containing green sand will meet the MCL for TCE if they are 1 m thick and the iron content is modest. For seepage velocities on the order of 1 m/day, a thick RB with high iron content is required to meet the MCL.

Acknowledgements

Financial support for this study was provided by the Wisconsin Department of Natural Resources (WDNR) and the Wisconsin Groundwater Research Advisory Council (GRAC), the latter administered by the Water Resources Institute at the University of Wisconsin-Madison. The findings in this paper are solely those of the authors. Endorsement by WDNR or GRAC should not be implied or assumed.

References

- [1] D. Blowes, C. Ptacek, J. Jambor, *Geoenvironment* 2000, 1995, GSP 46, 1588–1607.
- [2] A. Roberts, L. Totten, W. Arnold, D. Burris, T. Campbell, *Environ. Sci. Technol.* 30 (1996) 2654.
- [3] W. Arnold, A. Roberts, *Environ. Sci. Technol.* 32 (1998) 3017.
- [4] S. Benner, D. Blowes, C. Ptacek, *Ground water monitoring and remediation* 17 (1997) 99.
- [5] A. Francis, C. Dodge, Francis A., *Environ. Sci. Technol.* 32 (1998) 3923.
- [6] T. Shokes, G. Möller, *Environ. Sci. Technol.* 33 (1999) 282.
- [7] C. Su, R. Puls, *Environ. Sci. Technol.* 35 (2001) 1487.
- [8] G. Eykholt, D. Davenport, *Environ. Sci. Technol.* 32 (1998) 1482.
- [9] B. Koppensteiner, M.S. Thesis, University of Wisconsin, 1998.
- [10] J. Rael, S. Shelton, R. Dayaye, *J. Environ. Eng.* 121 (1995) 411.
- [11] D. Kershaw, S. Pamucku, in: J. Evans (Ed.), *In situ Remediation of the Geoenvironment*, ASCE, GSP 1997, vol. 71, pp. 26–40.
- [12] H. Moo-Young, T. Zimmie, *J. Geotech. Eng.* 122 (1996) 768.
- [13] D. Blowes, C. Ptacek, *Jambor, Environ. Sci. Technol.* 31 (1997) 3348.
- [14] K. Czurda, R. Haus, *Appl. Clay Sci.* 21 (2002) 13–20.
- [15] J. Kim, Ph.D. Dissertation, University of Wisconsin, 1996.
- [16] S. Bailey, T. Olin, M. Bricka, D. Adrian, *Water Res.* 33, (11) 2469–2479.
- [17] S. Javed, C. Lovell, Report JHRP/INDOT/FHWA-94/2J final report, Purdue School of Engineering, 1994.
- [18] T. Lee, C. Benson, *Geo Engineering Report 02–01*, University of Wisconsin-Madison, 2002.
- [19] J. Fort, MS Thesis, University of Wisconsin, 2000.
- [20] R. Starr, J. Cherry, *Ground Water* 32 (1994) 465.
- [21] D. Nelson, L. Sommers, *Methods of Soil Analysis*, Page, A., Miller, R., and Keeney, D. (Eds.), 539–579.
- [22] R. Zytner, *Water Air Soil Pollut.* 65 (1992) 245.
- [23] M. van Genuchten, *J. Hydrol.* 49 (1981) 213.
- [24] R. Freeze, J. Cherry, *Groundwater*, Prentice-Hall, Englewood Cliffs, NJ, USA, 1979.
- [25] D. Myrand, R. Gillham, E. Sudicky, S. O'Hannesin, R. John, *J. Cont. Hydrol.* 10 (1992) 159.
- [26] C. Chiou, D. Kile, D. Rutherford, *Environ. Sci. Technol.* 34 (2000) 1254.
- [27] G. Briggs, *J. Agri. Food Chem.* 29 (1981) 1050.
- [28] S. Karickhoff, D. Brown, T. Scott, *Water Res.* 13 (1979) 241.
- [29] Y. Shimizu, N. Takei, Y. Terashima, *Water Sci. Technol.* 26 (1992) 79.
- [30] K. Mayer, D. Blowes, E. Frind, *Water Resour. Res.* 37 (2001) 3091.
- [31] P. McMahon, K. Dennehy, M. Sandstrom, *Ground Water* 37 (1999) 396.
- [32] S. O'Hannesin, R. Gillham, *Ground Water* 36 (1998) 164.
- [33] R. Puls, D. Blowes, R. Gillham, *J. Hazard. Mater.* 68 (1999) 109.
- [34] S. Yabusaki, K. Cantrell, B. Sass, C. Steefel, *Environ. Sci. Technol.* 35 (2002) 1493.
- [35] J. Montgomery, *Water Treatment Principles and Design*, John Wiley, New York 1985.
- [36] J. Kim, J. Park, T. Edil, *J. Environ. Eng.* 123 (1997) 827.
- [37] S. Bin-Shafique, C. Benson, T. Edil, *Geo Engineering Report 02–014*, University of Wisconsin-Madison, 2002.
- [38] T. Johnson, M. Scherer, P. Tratnyek, *Environ. Sci. Technol.* 30 (1996) 2634.
- [39] T. Sivavec, P. Mackenzie, D. Horney, in: *Proceedings of International Containment Technology Conference*, U.S. DOE, U.S. EPA, and Dupont Co., 1997, pp. 753–759.
- [40] USEPA. *Treatability data base*, Water Engineering Research Laboratory, USEPA, Cincinnati, OH, 1990.
- [41] J. Mueller, S. Borchert, E. Klingel, D. Smyth, S. Shikaze, M. Tischuk, M. Brouman, in: *Proceedings of International Containment Technology Conference*, U.S. DOE, U.S. EPA, and Dupont Co., 1997, pp. 865–871.